A Thesis Presented to

The Faculty of Alfred University

DOPED BIOGLASS® MICROSPHERE CHARACTERIZATION AND ANALYSIS

by

Amber Smith

In partial fulfillment of
the requirements for
the Alfred University Honors Program

May 5, 2020

Under the Supervision of:

Chair: Dr. Anthony Wren Chair of Biomaterials Engineering

Committee Members:

Dr. Tim Keenan Professor of Biomaterials Engineering

Ms. Abby Griffith Director of the Judson Leadership Center

ACKNOWLEDGEMENTS

A special thank you to Dr. Anthony Wren and Dr. Tim Keenan for the endless support and guidance with this research. Abby Griffith, for being part of my thesis committee and significantly helping me refine my thesis. Dr. Stohr for his contributions of SEM data for this project. Also, Lauren Sleezer for her previous study and creation of material. Likewise, my friends and family for their infinite support and constant review of my work.

TABLE OF CONTENTS

LIST OF FIGURES AND TABLES

ABSTRACT

The creation of 45S5 Bioglass® microspheres and doped silver (Ag), copper (Cu), nickel (Ni) and zinc (Zn) 45S5 Bioglass® microsphere were completed via a torch flame process. Characterization included optical microscopy, R statistical modeling, X-ray diffraction (XRD), scanning electron microscopy (SEM) and energy dispersive spectroscopy (EDS). Optical microscopy allowed for color analysis and particle size measurements, specifically diameter, to be collected on the microspheres. This data was evaluated using R t-testing which determined that based on p-value dopants significantly effected microsphere size. Similarly, visual displays were created using R to support the statistics within a sample. XRD showed an amorphous sample with crystalline peaks. These peaks were aligned with the dopant of each glass. Shape, and surface assessment of the microspheres was examined using SEM. From the SEM images, the surface of the microspheres are not smooth and samples contained aspherical particles, but all contained many spherical particles. This characterization indicates better process controls need to be implemented. Additionally, through EDS, maps of dopant dispersion in the microspheres was obtained. From the surface, control 45S5 Bioglass® was evenly distributed containing all parts of the 45S5 composition but the dopants were not. Ag showed one dense location while other doped microspheres had varying distributions on the surface.

INTRODUCTION

Personal Background

First and most importantly I would like to give thanks for the endless support I have received from the Biomaterials Engineering (BME) Department and Alfred University. Dr. Wren and Dr. Keenan are not only wonderful professors but also offered encouragement and help always. Giving me and the BME's opportunities to learn. Similarly Ms. Griffith, her guidance through the JLC and WLA have truly changed my life. I am so grateful they were willing to be part of my honors committee. My friends have also had a huge impact on my thesis. Thank you for the virtual support: endless text messages, emails and reading over my work. Your positivity, comedic relief and encouragement is a blessing.

This project was of interest to me because of previous research I completed during my time at AU. Specifically, my research over the summer of 2018 focused on doping Bioglass®. The glass studied for this thesis was created very similarly to the method I had previously used. Likewise , similar dopants were studied. Beyond this, I was able to learn and help a graduate student friend during that summer. They were looking at doped Bioglass® microspheres for cancer treatment but he used a different doping process and dopants which were specific to cancer treatment. Still, I learned a lot about the process and was very interest in other microsphere applications and ways to manufacture them. I had debated continuing his research for my thesis before deciding on this project.

Personally, this work is very interesting to me. Before studying at Alfred University I had never imagined using glass inside the body. Through my studies I learned about how important Bioglass® is and how many diverse applications it has. Likewise, the founding story of why Dr. Larry Hench researched and discover Bioglass® is important as I have multiple friends and family members that are or were part of the military. (The story is explained later in the introduction.) I also am inspired by the idea that research like this could one day help people and reduce risks associated with disease, infection and cancer.

One key take away from this experience is the importance of being flexible and staying optimistic. I had looked forward to learning and developing my labs skills for bacteria culturing and cell growth during my thesis. Without the proper resources in the lab to do this my peers and I

decided to advocate for updates to our lab. We were persistence and worked hard as it was something we were excited and passionate about. The items needed to complete our research arrived right before break. Sadly, the COVID-19 situation intensified and resulted in us not returning to campus. This not only cut my research short but was disheartening as I was very excited for the lab skills development opportunity this thesis was going to provide. Yet, I learned new skills in regards to video conferencing, sewing, crocheting in addition to making many family memories.

The goal of this research was to determine horizontal oxygen-propane flame manufacturing reliability and effectiveness of 45S5 doped microspheres for antimicrobial properties. I have included literature review and background this topic to break down the history of similar work and the importance of why I researched this topic. This project was not completed due to the COVID-19 situation and still requires future work.

Bioglass® Conception

When a person thinks of glass typically windows, containers, bottles, and other similar objects come to mind. Yet, at the Larry Hench Memorial Symposium glass is the main topic and none of those objects are discussed. Bioglass® was discovered in 1969 by Larry Hench. This material was the first of its kind and allowed bonding of a synthetic material to occur within the body. Bioglass® is known as a biomaterial [1].

A biomaterial is a substance created to cure or replace, while enhancing, a biological aspect of a living animal. There are currently five generations of these materials. The first generation are called inert materials. The goal of these were to replace necessary aspects of the human body without harm. These inert materials have been around for centuries and were often made of metals and polymers [2].

The second generation, were considered bioactive. Bioactive is described by the ability of the material to permanently bond within the body. This was the generation of Dr. Hench's Bioglass®. Bioinert materials were known to cause fibrous encapsulation. Hench looked at why this occurred and made the key conclusion that materials used for the inert generation were not naturally found inside the body. Hench then looked to determine what was natural and how he could make a synthetic material that related [2].

In his research, hydroxyapatite (HA) became the key aspect. Hydrated calcium phosphate forms naturally in the body and growth of it on a synthetic material would allow the body to naturally

bond. The apatite layer forms between the tissue and the glass and this layer is what allows for the bonding to occur [2,3].

Hench discovered Bioglass® based on a request from a war medic. Who, at the time, served in the Vietnam war. It is only fitting that Hench's original research grant proposal was submitted to the US Army Medical R and D command and given a preliminary one year support. The research was originally conducted in vitro and then in vivo using rats. Results showed that the osteoblasts produced collagen fibrils which the hydroxyapatite connected to in layers. Thus, proving Hench's theory and lead to ten years of continued research support by the US Army. Beyond Bioglass® Dr. Hench developed many crucial technologies. This includes the cryogenic auger electron spectroscopy which he used for analyzing his Bioglass® discoveries. Hench did not just pioneer glass as a biomaterial but the research and technology that contributes to making such an invention [2].

Previous inert materials were aimed at replacing functional human facets. Thus, the materials used were based on physical properties. This is very important for function but didn't always provide a stable bond within the body. The HA bond brings immense strength and longevity, and moved the concept toward tissue regeneration and away from replacement. Bioglass® was determined to work for hard tissues such as bone. Dr. Wilson helped in this generation discovering that soft tissue would also allow HA formation and bonding using Bioglass®[2].

HA continues to be important and has been looked at in other biomaterial applications. There is many means of making HA synthetically, often in a powder form. Likewise, natural ways to derived it from animal bone. HA offers an ideal environment for osteo growth without toxic effects in biological applications [4]. HA forms by chemical and cellular reactions which is initiated in bone naturally in addition to the presence of Bioglass®. For this reason, Bioglass® is crucial to revive deteriorating bone. Deteriorating bone is seen in patients with osteoporosis and thus Bioglass® can be used to halt the progression of this disease [5].

Bioglass® is known for its specific composition. Based off weight percent, it is composed of 24.5 Na_2O, 24.5 CaO, 6.0 P_2O_5 and 45.0 SiO_2. From its composition, it also is known as 45S5. Some common brands that use this composition are NovaBone and Perioglas. Now, other glasses and glass-ceramics used in the medical industry have similar compositions. These materials include S53P4 used for AbminDent1 and BonAlive and A_W Glass-ceramic used in Cerabone [2,3].

The first official device using Bioglass® was the Ossicular Reconstruction Prothesis (MEP®) in 1985 which was followed by the Endosseous Ridge Maintenance Implant (ERMI®) in 1988 [2]. Since

then, huge strides have been made. The fifth, and current, generation looks at controlled drug delivery devices with emphasis on passive and active targeting [3].

Bioglasses are vital to the medical industry and still widely used, proven by the fact that they have a journal specifically dedicated to them known as the Biomedical Glasses Journal [2]. Bioglass® is even included in products such as toothpaste to help with mineralization [1]. Classically, the main applications include dental and orthopedic products. This includes coatings of Bioglass® and implants partly or completely composed of Bioglass®. Yet, new applications are being considered which includes blends of materials such as polymer and Bioglass®, wound healing and nerve regrowth. With the wave of the fifth generation, bioactive glasses are being evaluated for drug delivery functions. This application could be accomplished with microspheres [6].

Bioglass's® longevity in the market is due to its many valuable qualities. These include the ability to be used in areas utilized for load bearing and their strength is as strong as or stronger than natural bone. They form a bond in humans as soon as weeks with a bond thickness of up to 300 micrometers within 6 months and above all cause no toxic effects. There are limited studies showing the material's stability but so far it is estimated at least 10 years [2].

More notably, because of the ion exchange mechanism by which the creation of the bond forms, pH is changed within the area. This means that the material demonstrates bactericidal properties and thus allows it to be used in infectious areas of the body. Since discovery, changes to Bioglass® have been constant. Such as Dr. Yamamuro's and Dr. Kokubo's discovery of A/W to make a stronger composition [2].

Antibacterial Properties

Preliminary research has been completed to show that doping Bioglass® can enhance material properties and provide huge benefit to the patients. Typically, Bioglass® offer some antibacterial properties with the normal 45S5 composition. This means that patients have reduced risk and recovery time along with increase surgery success [6]. Research has demonstrated that normal Bioglass® can kill up to 55% of gram-positive bacteria and 80% of gram-negative [7].

Doping Bioglass® can further enhance these results. Lithium has shown it can be used to improve cell performance near the location of the implant and Cu dopant in Bioglass® is known to help with blood supply in the surrounding location while Zn studies have shown the potential to increase growth rate of bone. These preliminary studies and findings are being evaluated by many

researchers to better understand the true effects. Ag is one element proven in many applications to have antibacterial effects [6].

Bacteria is often found in wounds and can disturb healing or cause worse impacts such as death. Common bacteria in wounds are Staphylococcus aureus (S. aureus), Staphylococcus epidermidis (S. epidermidis), and Escherichia coli (E. coli). E. coli is considered a gram-negative bacteria while S. epidermidis and S. aureus are considered gram-positive. [7] The Bioglass® has the capabilities of killing these pathogens in a few different ways. From current understanding, ionic release is largely important because the ionic release changes pH. The membrane of bacteria degrades in high pH and the Bioglass® ionic release increases pH. Once the membrane of the bacteria is permeated the DNA and proteins can be destroyed thus killing the bacteria and making it ineffective and unable to harm. Likewise, the ionic release works with enzymes to cause similar effects. To augment this Bioglass® property, doping elements such as Ag, Cu, Zn, and strontium (Sr) are undergoing research [8,9].

One study shows that the addition of Ag in silica coatings killed 99.99% of S. aureus and E.coli after 24 hours. [9] Yet, studies show differing results because percentage of silver in the glass sample determines the antibacterial effect. High silver percentage increases the antibacterial effect. However, other aspects must be considered when increasing the dopant. Specifically, cell viability must be considered. The lack of viable cells in a bacteria free environment is still not effect for healing. Likewise, from a cost analysis perspective, overusing an element with no additional benefit is not efficient [10].

Metallic ions such as Zn and Cu could also be promising. Zn and Cu are found naturally in the body and are biologically active. Cu is important to metabolism and a majority of the body's Zn is located in bone. Specifically, Zn is densely found during bone formation, just before calcification and without proper amounts of Zn stunted bone growth can occur. In addition, both show promise in osteogenesis and angiogenesis. Bioglass® with these elements have the potential to be multifunctional and provide more stability in relation to deterioration of the Bioglass® when in a biological environment. Antibacterial effects of these elements have been seen in research with Zn in addition to anti-inflammatory effects proving to be successful in some in vitro testing. Although not proven, theoretically Cu should do the same [11,12].

Doping Bioglass® to provide antibacterial effects is promising and could revolutionize standard protocol. Beyond using metallic ions, others dopants are being considered for antibacterial

properties. Chitosan, a naturally derived material, is being used for inhibitory effects in regards to bacteria. Chitosan has proven to be effect alone in killing bacteria surrounding the particles. That is, only killing bacteria interfacing with the Chitosan. Research of doped Bioglass® with Chitosan, Bioglass® Chitosan compositions and a Bioglass® Chitosan composition doped with metallic ions are being pursued for effectiveness [13].

Microspheres

Bioglass® can be formed in many ways for implantation. Scaffolds are a technique used which provide a porous environment. Figure 1 shows a glass scaffold structure. Better, they can be loaded with cells and proliferation materials which enhance growth once implanted. Production includes dry-powder processing and foam fabrication. Another way to implant Bioglass® is by using microspheres [14,15].

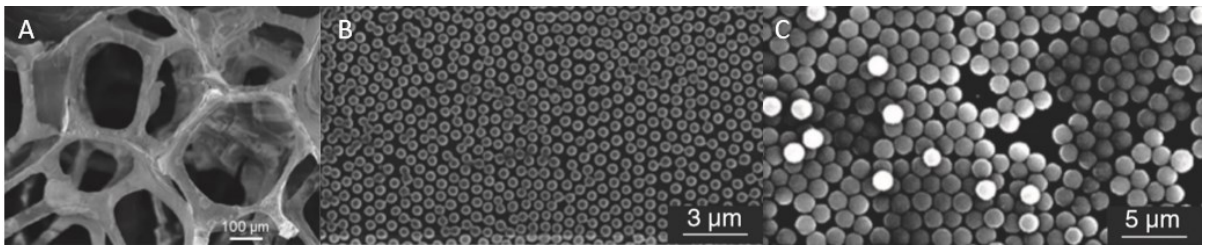

Figure 1. Literature Images of A) 3D Glass Scaffold[15] B) Polymeric Microspheres[16] C) Polymeric Microspheres[16]

Microspheres can be polymeric, ceramic, glass, among other materials. The principle is a completely spherical particle that is homogeneous. When producing these particles, statistical standards are used to determine the dispersion of a batch with aim to be monodispersed. Exploration of improved production methods and new applications for microspheres is being determined. There particles can be produce from a material that is in powder form using thermal processing, plus though emulsion or droplet formation to name a few. Each process is used for different applications and starting material [16].

Specifically, Bioglass® can be processed thermally to form microspheres. When converting Bioglass® careful attention to temperature and conversion is key. Amorphous Bioglass® is known to become crystallin during temperature change. Thus, thermal processing of the Bioglass® to create

microspheres can alter the structure. Bioglass® is functional in a crystalline state but often is not as effective because it has a reduced HA transition rate. As a result of the crystalline state, bone calcification is slower [17].

Bioglass® microspheres offer a range of applications including chromatography, drug delivery devices, orthopedic uses including bone tissue engineering and cancer treatment [16,18,19]. Cancer treatment using microspheres would allow for a less invasive treatment. Injecting the microspheres into a tumor and using other medical equipment to cause their rotation would allow for precise heat for a specific area. This heat would be used to kill the tumor cells. As tumor cell death occurs at a lower temperature than normal cells this would be ideal for not harming healthy cells. Furthermore, radioactive microspheres can be used for a similar application [19].

45S5 Bioglass®

The Bioglass® used in this research was synthesized by Lauren Sleezer. The composition used was the typical 45S5 distribution. Specifically, 41.895g Na_2CO_3, 43.725g $CaCO_3$, 9.725g NH_6PO_5 and 45.0g SiO_2. The powder was roller mixed for 2 hours and melted for an hour at 1300˚C using a Lindbery Blue Box furnace. Ms. Sleezer used the shock quench method followed by milling. The final Bioglass® size was 125µm [20].

Bioglass® Microspheres

The Bioglass® was then processed into microspheres. This process was completed inhouse using a homemade system. An oxygen-propane flame with a temperature of about 3000˚C projected horizontally. A vibrating spatula resided over this flame and shook the Bioglass® off the spatula into the center of the flame. From there, the flame carried particles into a collection area. This process is depicted by Figure 1 shown below [20].

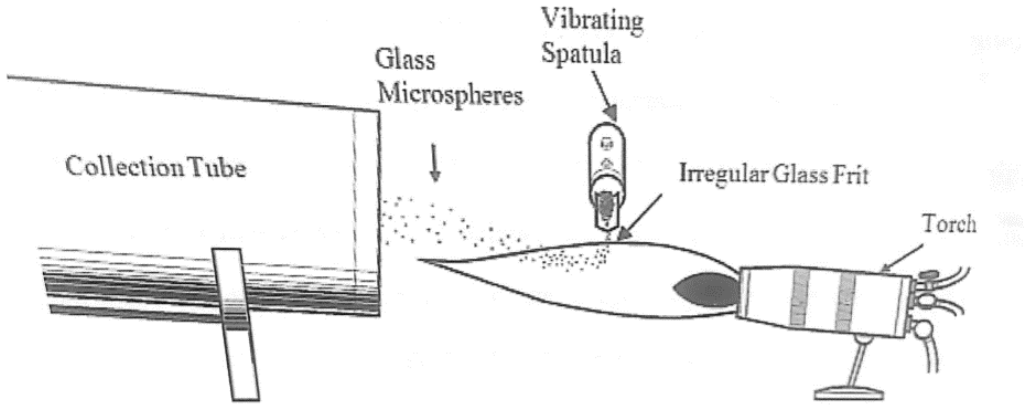

Figure 2. Microsphere Synthesis Set Up[20]

To dope the Bioglass® the same synthesis process was used. Yet, previous to placing the Bioglass® powder onto the vibrating spatula, one gram of Ag_20, CuO, NiO or ZnO were mixed with five grams of Bioglass® for each sample. A milling process was used to ensure a proper mix occurred [20].

Leica Microscope

Using AS V4.8 imaging software and a Leica M165 FC Optical Stereomicroscope images of all microsphere samples were collected. The images were gathered at 5X and 12x magnification. The samples were mixed in their collection container for 1 minute, by hand, and each placed into separate 47mm petri dishes as well as a small white weigh boats to acquire these images.

Olympus Microscope

At 4X magnification, an Olympus IX20-UCB Optical Fluorescence Microscope was used to obtain images which were then analyzed using Image-Pro AMS 5.1 software. As with the Leica, the samples were mixed in their collection container for 1 minute, by hand, and each placed into separate 47mm petri dishes. The analyzing software was used to measure the diameter for each microsphere sample, about 125 diameters of each sample were measured. This process allows for assessment of size which was completed using R-programing.

R-Programing

Using R-programming language Version 3.6.2, 275 diameters of each type of Bioglass® microsphere were analyzed. Code was used to produce a Boxplot and a Violin plot. Likewise, an interactive html file was produced to gather specific data not displayed on the graphs. This includes minimum, maximum, Q1, Q3, median and the upper fence.

Also, to show trends in size and the significance compared to the other samples a statistical analysis was completed using a t-test. The t-test was based on a null hypothesis which states that the means are equal. The alternative hypothesis states that the means are not equal. To tell the significance p-value and confidence interval were looked at. In regards to the p-value, the smaller the p-value the more likely the alternative hypothesis is significant. Furthermore, to compute this, the standard deviation, variance and mean were determined through the code.

Scanning Electron Microscope (SEM)

Images were also captured using a JEOL 7800F SEM. To prepare the samples for imagining, the samples were mixed in their collection container for 1 minute, by hand. Imaging studs with carbon tape were then dipped into the spheres. To reduce charging, each sample was gold coated. EDS was completed on each sample using an Octane Plus detector and TEAM software.

X-ray Diffraction

Data were collected on a Bruker D2 Phaser diffractometer in Bragg-Brentano geometry using a plastic zero-background sample holder. Grinding or other manipulation of the specimen was not completed. The samples were mixed in their collection container for 1 minute, by hand before being placed into the sample holder. Ambient atmosphere was used and the measurement conditions of 10°2θ to 70°2θ, step size of 0.02˚2θ and 2.0 seconds count time. Bruker DIFFRAC.SUITE software was utilized. Specifically, DIFFRAC.EVA and PDF-4+ software to perform phase ID on each sample.

Agar Bacteria Testing

Escherichia coli, Staphylococcus aureus, and Staphylococcus epidermidis were grown in Luria-Bertani (LB) broth, nutrient broth and Tryptic Soy (TS) broth respectively for 24 hours at 37˚C to create stock cultures. It was intended that these cultures would be used to prepare agar plates.

Intended procedure was to use the stock cultures to make dilutions which would be used in testing. 20µL of the stock culture would be mixed with 980µL of sterilize deionized water and 50µL of the stock culture would be mixed with 950µL of sterilize deionized water. These samples would be vortexed for approximately one minute. Following this, sterile cotton swabs would be dipped into the diluted samples and then swabbed across each agar plate.

The agar plates would contain 20ml of Luria-Bertani (LB) agar, nutrient agar or Tryptic Soy (TS) agar. Making two plates, one for the 2% dilution and one for the 5% dilution of bacteria, for each agar type and for each sample. A total of 30 agar plates would have been created. Once swabbed with the bacteria dilutions, microspheres would be sprinkled, using gloved fingers, over the plate. Prior to plating, the microspheres were autoclaved to sterilize.

Optical Microscope

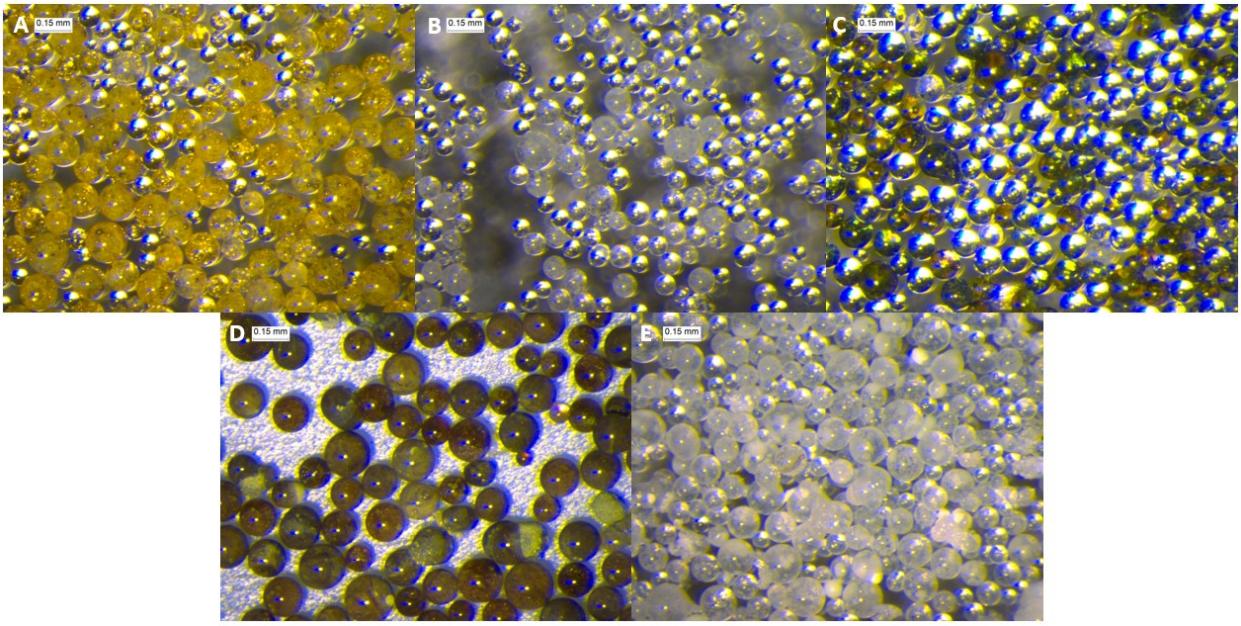

Figure 3. Optical Stereomicroscope images of microsphere sample A) Ag Bioglass® B) Control Bioglass® C) Cu Bioglass® D) Ni Bioglass® E) Zn Bioglass®

Figure 2 shows Optical Stereomicroscope images for all samples. From these images presence of the dopant can be confirmed based on color. The Ag sample (A) appears yellow, Control (B) clear, Cu (C) green, Ni (D) brown, and Zn (E) white. Without a dopant present all samples would be clear. The images above were gathered at 5X magnification and gives insight to sample shape. Accordingly, the samples appear spherical as intended. At 12x magnification the images portrayed the same color but clearly showed that not all microspheres were spherical. SEM images were gathered to further investigate the shape.

Olympus

Images were collected at 4X magnification as seen in Figure 3. These optical images were analyzed in Image-Pro AMS 5.1 software. This allowed the diameter of microspheres to be measured for each sample. 125 diameters of each sample were taken. Figure 4 illustrates this process. Multiple images were taken to accurately measure microsphere diameter and each image was analyzed

separately. Only microspheres that appeared spherical were measured. From these images it is clear that the size of the microspheres are not uniform. Furthermore, that the dopant affected the size of the microspheres. The data collected was compiled for each sample type. Additionally, data from a previous experiment for each sample type was included. This was an additional 150 diameters for each sample. This process allowed for assessment of size which was completed using R programing.

Additionally, these images indicate also that not all samples are spherical and that particles of oxide still remain mixed with the microspheres. This is clearly seen in Figure 3 E as small pieces of material surround the microspheres. This was further investigated using SEM. To reduce this, the microspheres could be sieved to eliminate a majority of oxide particles without eliminating microspheres.

Research indicates that the glass particle size entering the flame directly effects the amount of spherical particles. Smaller glass frit produces a more spherical output. Investigation of this topic shows that this is due to the time it takes for a particle to complete spheroidization. Larger particles take longer for this process and thus a mixed composition of spherical particles, glass frit, and aspherical particles is seen after processing [18]. The Zn Bioglass® has this mixed composition and as seen in Figure 3 E and data collected via the optical microspheres and analyzed with R the Zn microspheres were the largest. This could suggest that the input glass frit and dopant were larger compared to the other batches.

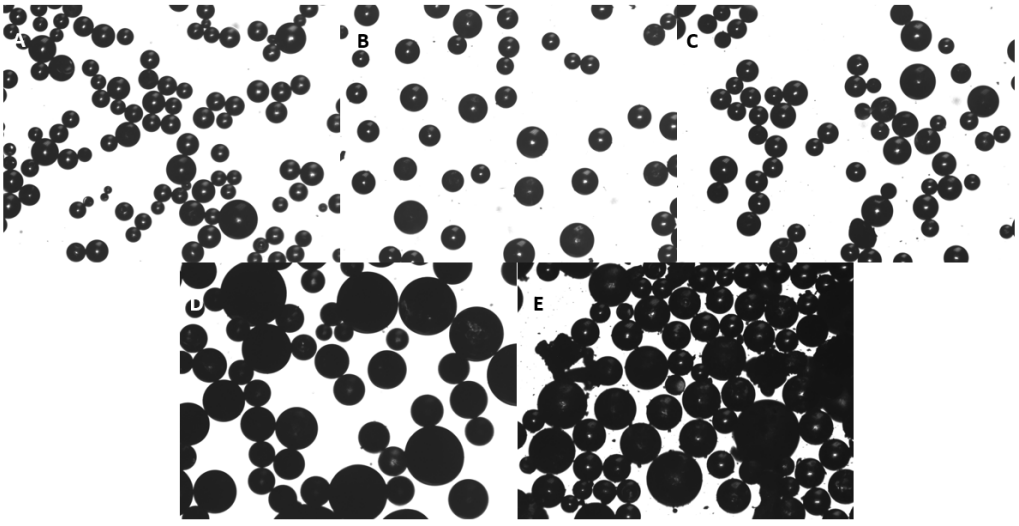

Figure 4. Optical Fluorescence Microscopy images of microsphere sample A) Ag Bioglass® B) Control Bioglass® C) Cu Bioglass® D) Ni Bioglass® E) Zn Bioglass®

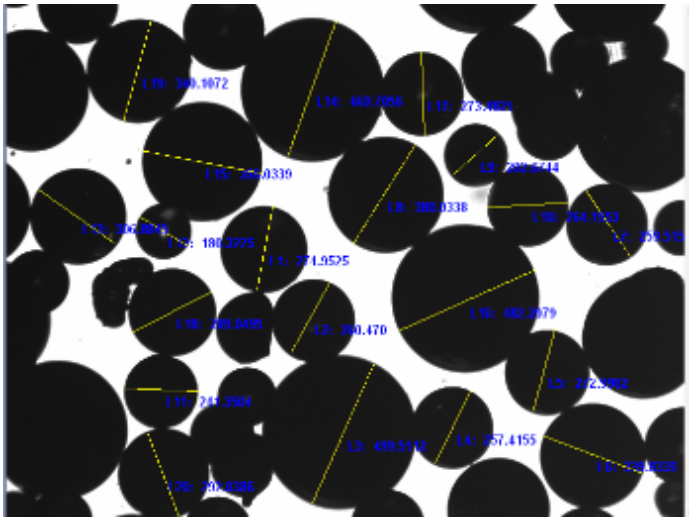

Figure 5. Image-Pro AMS 5.1 software measurements of Control Bioglass® microsphere sample

R Programing

Size analysis was conducted to determine how each microsphere relates within its sample group and T-testing was completed to compare how each microsphere size relates to other samples.

T-test

To prove the t-test is significant and the alternative hypothesis is true based on a 95% confidence interval, the p-value must be less than 5% (0.05). Likewise, the confidence interval cannot contain 0. If these qualifications are not met then the t-test is not significant and the null hypothesis is true. This would show that the mean diameter for two microspheres when compared are equal and are within the confidence interval with 95% confidence.

After completing this test for my data, the results show that all microsphere types have diameters that are significantly different from each other. This means that with 95% probability, if 100 microspheres of two different types are measured for their diameters, only 5 of the microspheres would have similar diameters. Thus, showing that there is a high chance that they will have significantly different diameters. This is further signified because 0 is not in the confidence interval.

Violin Plot

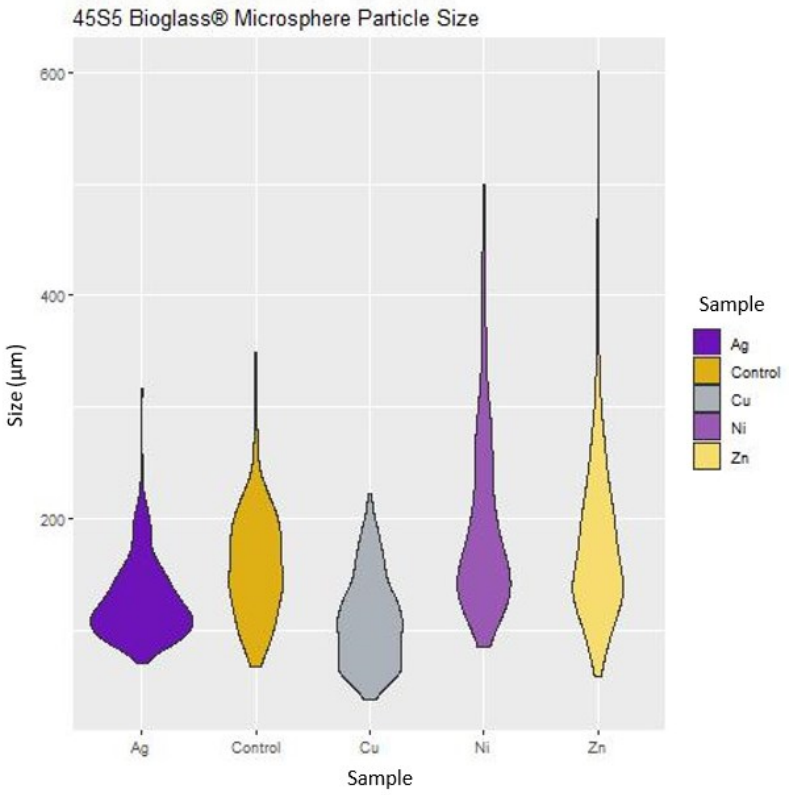

Figure 6. Violin Plot

In addition to the data a box plot provides, a violin plot shows density of the data within a sample. This helps identify how many values lie in a specific range of sizes for a given population. Thus, helping identify if your data has a multimodal distribution. The thinner areas of a violin plot show few data points within that size range. The thicker areas show that multiple data points lie within that range. For multimodal distribution, two or more similar thick areas are shown in a sample. This implies it has two different modes, peaks, within the same data set. These modes have unique medians and don't represent the entire data but rather the median for the specific mode. A box plot would show a median for the entire data set and thus not identify this.

Seen in Figure 2, all samples are unimodal. That demonstrates that the median given by the box plot data represents the entire data set accurately. Furthermore, it shows that the microspheres have nearly a uniform reaction to the dopant.

Although not specifically determined, the longitude of the violin plot for each sample is likely more a result of the microsphere processing. This can be identified due to the longitude of the control sample. If it was based on the dopant the control would not have a long violin plot. Although, the 45S5 Bioglass® was sieved to a specific size, when processing it varying amounts fall into the flame at a given time. Likewise, the sieved glass falls into different areas of the flame regardless of the attempt for it to fall directly into the center of the flame. As a result, the size varies.

Box Plot

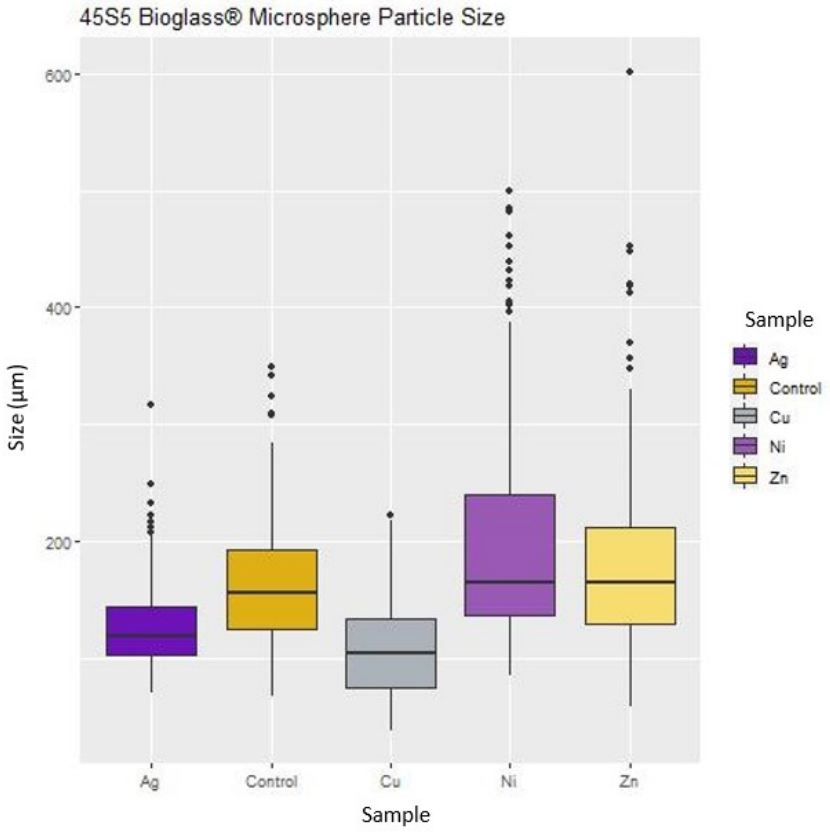

Figure 7. Box Plot

In Figure 1, the box plot describes statistically the diameter of each Bioglass® microsphere sample. It show four quartiles. The box describes three of the quartiles. The top of the box represents quartile 3, the middle line in the box represents quartile 2 and the bottom line forming the box represents quartile 1. Each signifies a median. With quartile 2 being the median of the entire data set. The whiskers, seen as the lines exiting the box, also explain the data. The top, of the whisker above

the box, shows the upper fence with the bottom of the lower whisker showing the minimum value in that samples data set. The black dots for each sample indicate outliers in the data. This shows how the diameters of the microsphere samples are distributed.

This plot identifies that all samples have outliers. Likewise, that the data points in Ni and Zn have a large range. On the opposite side, Ag has a smaller range in datapoints than the control. This can be seen due to the width of the box. Multiple reasons could contribute but as identified in the violin plot, it is likely due to processing.

Table 1. Particle Size Analysis

Sample	Ag	Control	Cu	Ni	Zn
Min	69.78	66.90	36.94	84.01	57.95
Q1	101.58	123.76	74.68	135.56	128.63
Mean	126.63	159.89	108.68	195.23	177.76
Median	118.97	155.70	104.02	164.27	163.79
Q3	143.89	192.04	132.87	239.73	212.05
Upper Fence	207.21	283.44	216.87	386.84	329.55
Max	316.63	348.89	222.07	500.38	602.18
Standard Deviation	35.12	50.81	40.48	85.82	74.37
Variance	1233.45	2581.39	1638.31	7365.66	5531.00

Table 1 shows the values generated by the plots for each sample. Likewise, it shows the values computed to complete t-tests for each sample. The data shows that the smallest microsphere diameter was recorded for the Cu microspheres. The largest diameter was recorded for the Zn microsphere.

Research of titanium phosphate glass microspheres shows that particle size distribution is due to processing techniques regardless of composition. This research demonstrates that the glass powder size and the flame are important factors in microspheres. The variables associated with our processing could have resulted in the above data. Research on the phosphate glass indicates that these variables could include the temperature and size of the flame plus the location of the powder within the flame causing variable times which the particle resided in the flame[18].

SEM

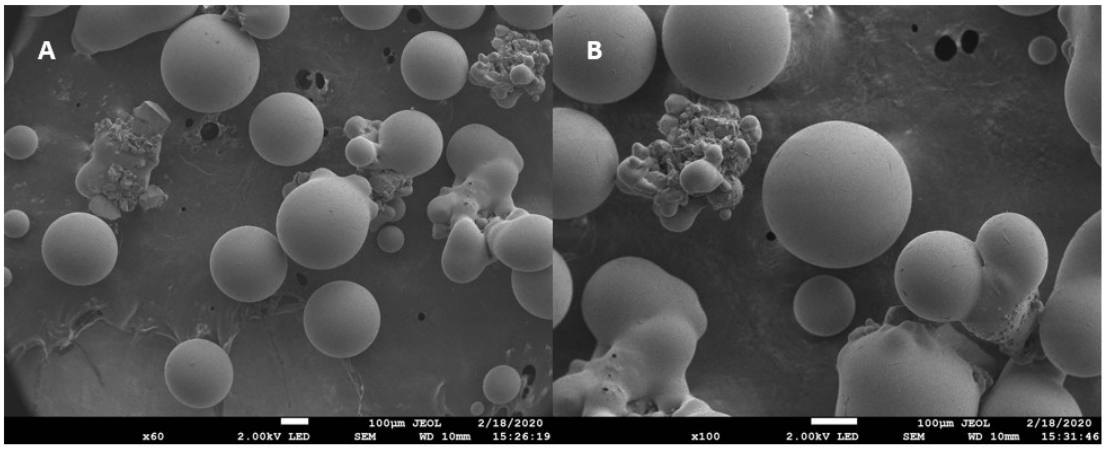

Figure 8. JEOL 7800F SEM images of Control Bioglass® sample A) 60X B) 100X

Figure 7 shows the Control Bioglass® at a magnification of 60X and 100X. These SEM images display the shape of the microspheres. Microsphere creation can be confirmed from these images. Multiple similar sized spherical particles are seen. Yet, the images indicate that processing of microspheres is not ideal. This can be seen from the particles that do not resemble a spherical shape. Likewise, some particles are spherical but connected demonstrating the need for further process and collection controls.

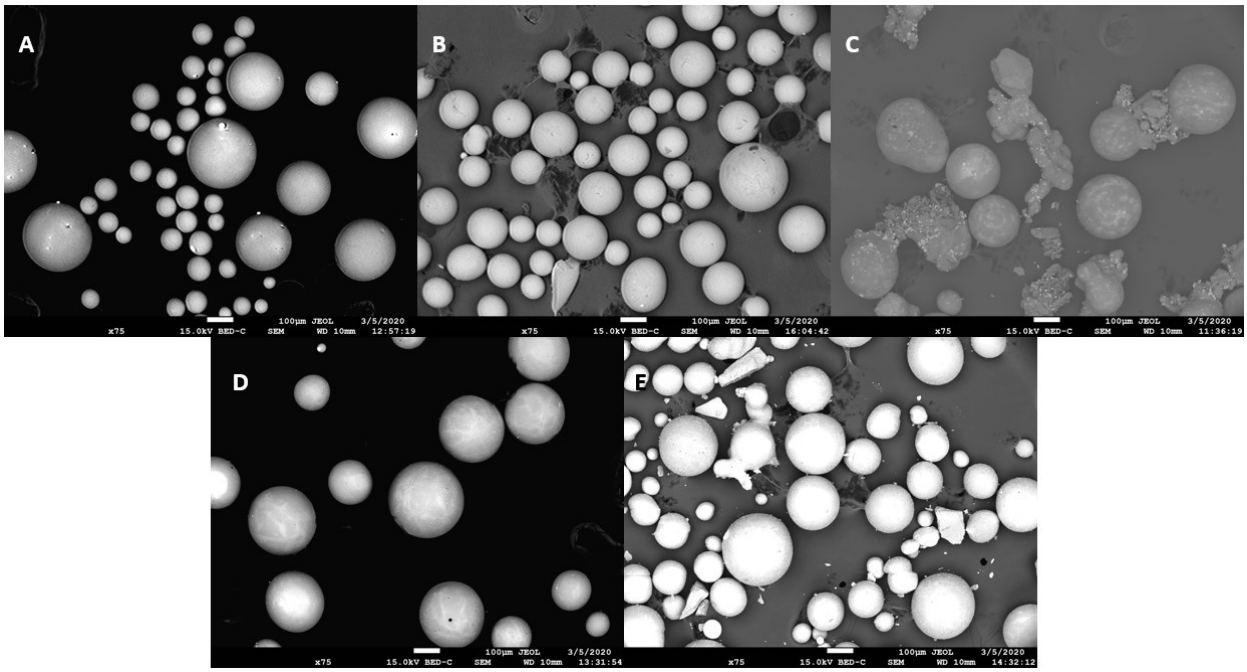

Figure 9. JEOL 7800F SEM images of microsphere sample A) Ag Bioglass® B) Control Bioglass® C) Cu Bioglass® D) Ni Bioglass® E) Zn Bioglass®

SEM images at a magnification of 75X for each sample are shown in Figure 8. These images visually supplement the size analysis completed and visual confirm that each Bioglass® sample size is different. Likewise, the microsphere size for a specific sample ranges and includes outliers. Images further showed all samples do have residual powder from creation and deformed particles that to don't represent the spherical shape intended.

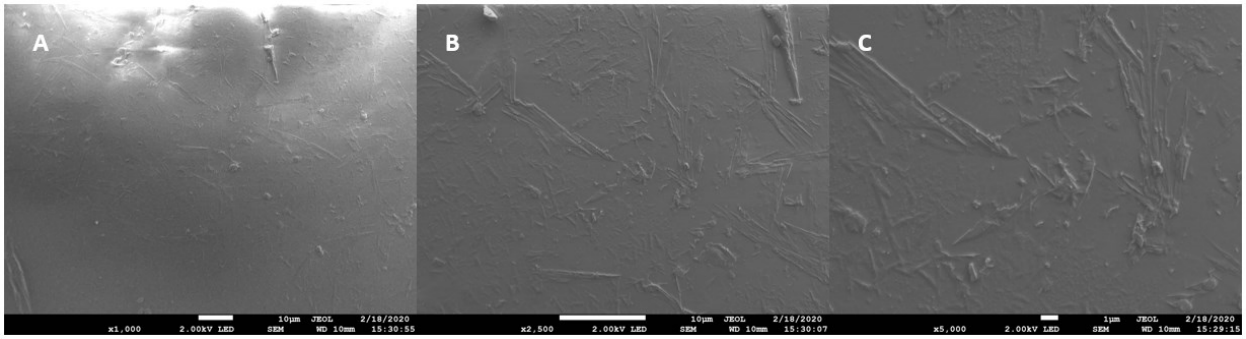

Figure 10. JEOL 7800F SEM images of the Control Bioglass® microsphere sample surface A) 1000X B) 2,500X C) 500X

Images at magnification of 1000X, 2,500X and 5,000X where also observed to allowed analysis of surface texture. Aimed surface characteristics were smooth but observed is an varying texture. This texture is seen over much of the surface and can be seen as differing line outdents.

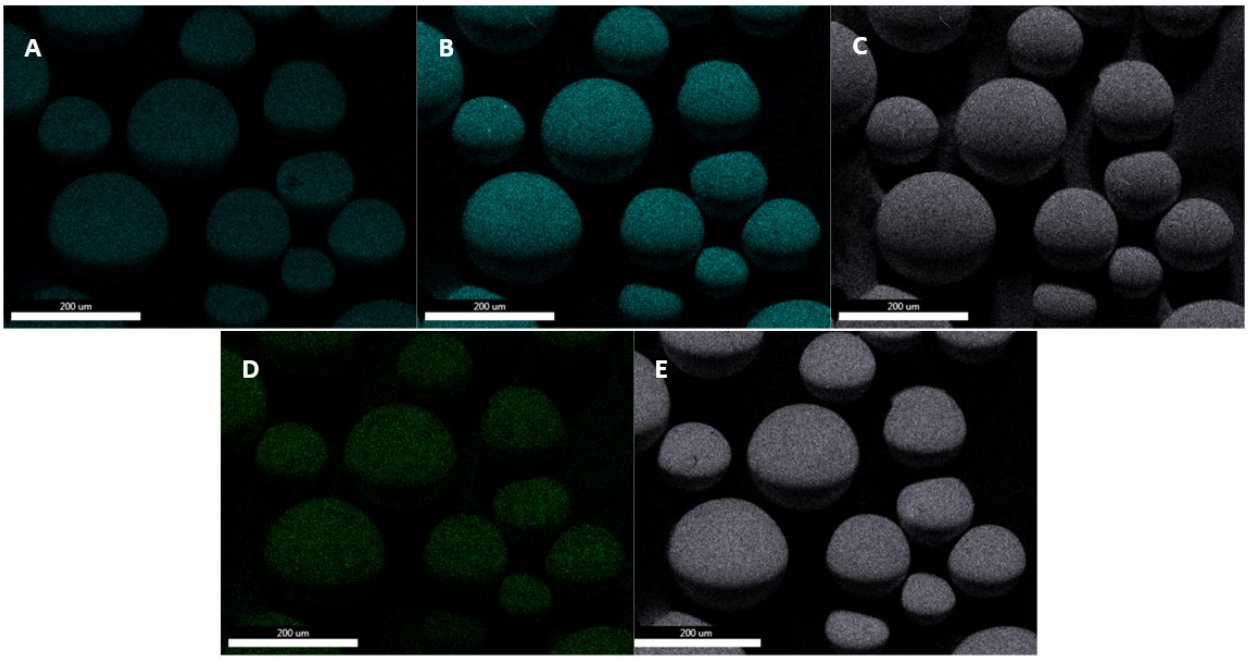

Figure 11. EDS of the Control Bioglass® microsphere sample using a JEOL 7800F SEM showing composition A) Ca B) Na C) O D) P E) Si

An Octane Plus detector and TEAM software were used to complete the EDS map seen in Figure 10. The Control Bioglass® microsphere sample was mapped. The components Ca, Na, O, P, and Si, as intended, were identified in each control microsphere. Distribution of these elements is even on the surface. The EDS map in Figure 10 doesn't indicate and even distribution of elements at the center of the microsphere. To better understand distribution throughout the microsphere, the spheres could be crushed and placed in carbon paste. Thus, EDS mapping of the inside of the sphere could be completed and indicate the distribution of elements.

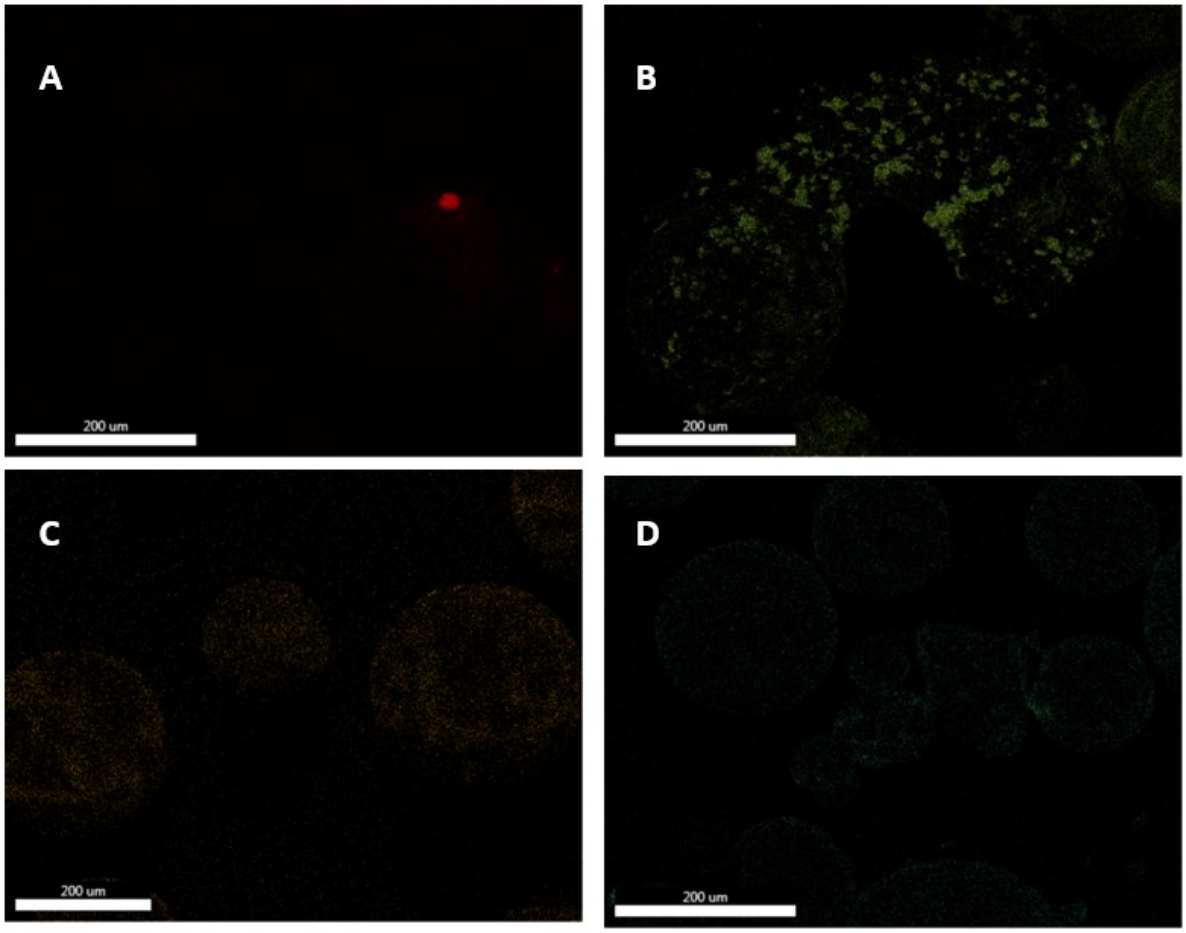

Figure 12. EDS of the Bioglass® microsphere samples using a JEOL 7800F SEM showing doped composition A) Ag B) Cu C) Ni D) Zn

Similarly, the EDS mapping of the dopants in Figure 11 can only indicate presence of the dopant on the surface. In all compositions, the dopant was identified. Yet, the identification is very faint. This is due to the very small mole percent, about 1%, of dopant. Furthermore, the dopant is not evenly distributed in any sample. In the Ag sample, one dense and large Ag spot can be seen on the surface. In other samples, the dopant is in higher concentration in one area compared to another. EDS mapping of the doped samples indicates that the doping process must be changed for a replicable and balanced sample.

X-ray Diffraction Analysis

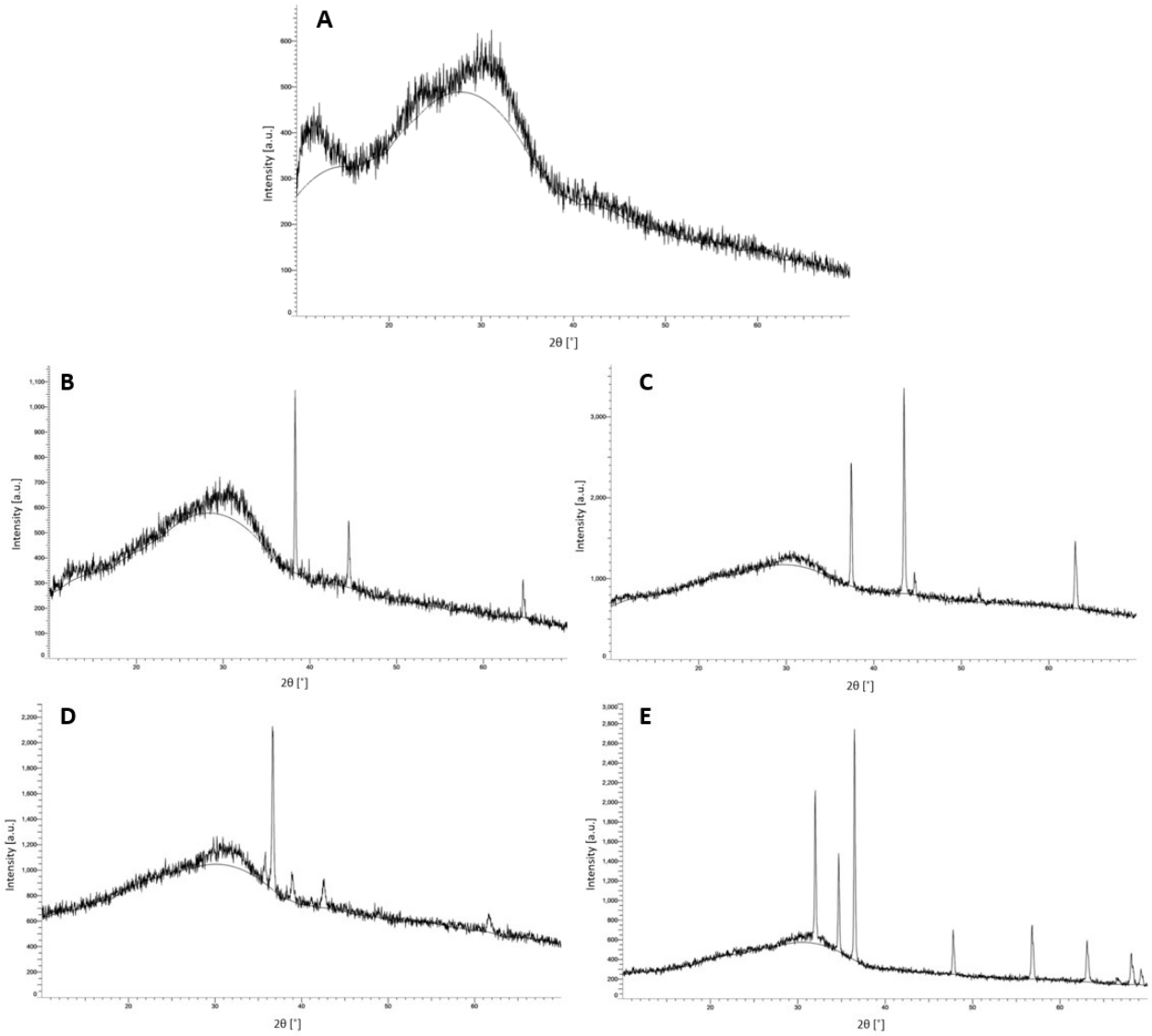

Figure 13. XRD for Bioglass® microsphere samples A) Control Bioglass® B) Ag Bioglass® C) Cu Bioglass® D) Ni Bioglass® E) Zn Bioglass®

X-ray diffraction data was collected using a D2 Phaser. Once collected, Bruker DIFFRAC.SUITE software was utilized. Specifically, PDF-4+ software was used to perform phase ID of the crystalline peaks on each sample. PDF files were matched to the XRD patters for each sample visually. PDF card 00-004-0783 was matched with XRD B and signifies silver, PDF card 00-005-0667 was matched with XRD C and signifies cuprite, PDF card 01-089-3605 was matched with XRD D and signifies lithium

nickel oxide, and PDF card 01-080-3508 was matched with XRD E and signifies Nickel Zinc Oxide. Cuprite is a cuprous oxide. The dopant is expected to be identified in an oxide form as oxygen was present in the formation process. Yet, identifying silver and not silver oxide in XRD B was not expected. This could mean that the large dense particle seen in the EDS map is solid silver. Thus, silver particles formed and attached to the microsphere surface in the doping process. All of the PDF files match the intended dopant confirming doping occurred for each sample. The X-ray diffraction patterns also include an amorphous hump for each sample. Typically, a Bioglass® is considered amorphous.

Literature review suggests that a fully amorphous doped silver glass can be obtained. A SiO_2 glass was used for this experiment which means that a similar result could be obtained for Bioglass®. Different processing was used, specifically the Stöber method [19].

Antimicrobial Testing

Antibacterial work was started but not completed. A preliminary test was done using two 20ml plates of LB agar. One of each E.coli dilution, 2% and 5%, was used on separate plates. Sterile Ag microspheres were sprinkles over the top and incubated for 24hrs at 36˚C. After visual inspection, the E.coli didn't grow around the microspheres. This data was only visually examined. Furthermore, the E.coli was not spread evenly over the plate.

The research focused on Ag doped SiO_2 glass (Si/Al/Ag = 1/0.01/0.01) also demonstrated antibacterial properties occur against E. coli with the microspheres. These results indicated that the current commercial properties of antibacterial products using Ag is twice as effective. Thus, opportunity for improvement is present. Ion release also occurred in these samples [19].

CONCLUSIONS

Doped microspheres offer the ability to reduce infection and increase recovery time. Characterization techniques showed that the oxygen-propane torch processing method creates applicable microspheres. Yet, the research indicates that further process controls are required to achieve more uniform production of samples. This was seen by both R-programing analysis which shows large ranges in the diameters of microspheres in each sample and visually in the SEM images where varying particle shapes and original glass powder is seen. Likewise, using this process is effective in doping microspheres but the true distribution of the dopant within the sample is unidentified. Furthermore, XRD data shows the need to research changes to the process which would allow for a completely amorphous doped sample. To understand the real applicability of antimicrobial doped microspheres proper bacteria and cell testing must be completed.

FUTURE WORK

Due to the COVID-19 situation, no bacteria or cell testing was completed for this research. It is crucial that these are completed. Bacteria testing will determine if the dopant is effective in killing bacteria. The common infection bacteria, S. aureus, S. epidermidis, and E. coli, should be evaluated for each sample. Recording and analyzing of the inhibition zone data will provide evidence of the antibacterial effect. In addition, cell growth in the presence of the microspheres must be researched. Fibroblasts and osteoblasts are essential to successful implantation. Evidence of their ability to grow in the presence of microspheres would support effectiveness. In the long run, in vivo testing must be complete. Systemic and long term effects of the doped Bioglass® would be assessed as part of this study.

In addition, process controls for manufacturing the microspheres must be improved. To reduce aspherical shapes the powder must enter the center flame in smaller quantities and stay within the flame for an extended time. This can partly be done by improving the mechanism used to create the particles and using fixed settings to get easily repeatable results.

To reduce a large range in particle size sieving can be used after the microspheres are created. Excess powder and aspherical shapes will also be decreased in this process. Understanding the effects of changing the glass particle powder size used to make the microspheres is important to better understand possible applications.

Doping technique review would allow for a better understanding on how to create a uniform coating. EDS mapping of inside the microsphere particle would give understanding to the distribution of elements throughout the microsphere rather than solely surface understanding.

Understanding the strength and durability of the microsphere would help determine possible applications including the ability of doped microspheres to have drug delivery potential. In addition, ion release should be assessed. Understanding the degradation of the material and the elements it is doped with will help determine short and long term systematic effects on the body.

REFERENCES

1. D.S Brauer and J.R. Jones, “Special Section of Papers Presented at the Larry L. Hench Memorial Symposium on Bioactive Glasses at the Annual Meeting of the Glass and Optical Materials Division of the American Ceramic Society,” Biomedical Glasses, 2 [1] 49-50 (2016).

2. L.L. Hench, “Opening Paper 2015- Some Comments on Bioglass: Four Eras of Discovery and Development,” Biomedical Glasses, 1 [1] 1-11 (2015).

3. L.L Hench and J.R. Jones, “Bioactive Glasses: Frontiers and Challenges,” Front. in Bioeng. Biotechnol., 3 [194] 1-9 (2015).

4. M. Lombardi, P. Palmero, K. Haberko, W. Pyda, and L. Montanaro, “The Contribution of Natural Hydroxyapatite to the Development of Bone Substitutes,” Key Engineering Materials, 541 3-14 (2013).

5. L.L. Hench, N. Roki, and M.B. Fenn, “Bioactive Glasses: Importance of Structure and Properties in Bone Regeneration,” Journal of Molecular Structure, 1073 24-30 (2014).

6. V. Miguez-Pacheco, L.L. Hench, and A.R. Boccaccini, “Bioactive Glasses Beyond Bone and Teeth: Emerging Applications in Contact with Soft Tissues,” Acta Biomaterialia, 13 1-15 (2015).

7. S. Hu, J. Chang, M. Liu, and C. Ning, “Study on Antibacterial Effect of 45S5 Bioglass®,” Journal of Materials Science: Materials in Medicine, 20 [1] 281-286 (2009).

8. J.S. Fernandes, P. Gentile, R.A. Pires, R.L. Reis, and P.V. Hatton, “Multifunctional Bioactive Glass and Glass-Ceramic Biomaterials with Antibacterial Properties for Repair and Regeneration of Bone Tissue,” Acta Biomaterialia, 59 2-11 (2017).

9. S. M. Lee, B. S. Lee, T. G. Byun, and K. C. Song, “Preparation and Antibacterial Activity of Silver-Doped Organic–inorganic Hybrid Coatings on Glass Substrates,” Colloids and Surfaces A: Physicochemical and Engineering Aspects, 355 [1-3] 167-171 (2009).

10. M. Catauro, F. Bollino, F. Papale, and S. V. Ciprioti, “Investigation on Bioactivity, Biocompatibility, Thermal Behavior and Antibacterial Properties of Calcium Silicate Glass Coatings Containing Ag,” Journal of Non-Crystalline Solids, 422 16-22 (2015).

11. Cacciotti, “Bivalent Cationic Ions Doped Bioactive Glasses: The Influence of Magnesium, Zinc, Strontium and Copper on the Physical and Biological Properties,” J. Mater. Sci., 52 [15] 8812-8831 (2017).

12. P. Balasubramanian, L.A. Strobel, U. Kneser, and A.R. Boccaccini, “Zinc-Containing Bioactive Glasses for Bone Regeneration, Dental and Orthopedic Applications,” Biomedical Glasses, 1 [1] 51-69 (2015).

13. M. Kong, X.G. Chen, C.S Liu, C.G. Liu, X.H. Meng, and L.J. Yu, “Antibacterial Mechanism of Chitosan Microspheres in a Solid Dispersing System Against E. Coli,” Colloids and Surfaces B: Biointerfaces, 65 [2] 197-202 (2008).

14. Q.Z. Chen, I.D. Thompson, A.R. Boccaccini,“45S5 Bioglass®-Derived Glass–ceramic Scaffolds for Bone Tissue Engineering,” Biomaterials, 27 [11] 2414-2425 (2005).

15. F. Baino, E. Fiume, M. Miola, E. Verne, “Bioactive Sol-gel Glasses: Processing, Properties, and Applications,” Int. J. Appl. Ceram. Technol. 15 841-860 (2018).

16. J.C De La Vega, P. Elischer, T. Schneider, and U.O. Hafeli, “Uniform Polymer Microspheres: Monodispersity Criteria, Methods of Formation and Applications,” Nanomedicine, 8[2] 265-285 (2013).

17. H. Fu, M.N Rahaman, D.E. Day, and W. Huang, “Long-Term Conversion of 45S5 Bioactive Glass–ceramic Microspheres in Aqueous Phosphate Solution,” J. Mater Sci.: Materials in Medicine, 23 [5] 1181-1191 (2012).

18. N.J Lakhkar, J Park, N.J. Mordan, V. Salih, I.B. Wall, H Kim, … J.C. Knowles, “Titanium Phosphate Glass Microspheres for Bone Tissue Engineering,” Acta Biomaterialia, 8 [11] 4181-4190 (2012).

19. M. Kawashita, “Ceramic Microspheres for Biomedical Applications,” International Journal of Applied Ceramic Technology, 2 [3] 173-183 (2005).

20. Lauren Sleezer, “Synthesis, Characterization, and Antibacterial Efficacy of Silver, Copper, Nickel, and Zinc Doped Bioglass® Microspheres.” BS. Thesis, Alfred University, Alfred, NY, 2019.